https://doi.org/10.18321/1102

Factors Influencing the Kinetics of Water Vapour Adsorption on Activated Carbons

Y. Boutillara[1,2], L. Richelet[1], L.F. Velasco[1]*, P. Lodewyckx[1]

[1]Department of Chemistry, Royal Military Academy, Avenue de la Renaissance 30, Brussels, Belgium
[2]Unité d'Enseignement et de Recherche en Physico-chimie des Matériaux / Ecole Militaire Polytechnique, B.P 17, Bordj El-Bahri, 16046, Algiers, Algeria

Article info

Received:
25 January 2021

Received in revised form:
5 March 2021

Accepted:
26 April 2021

Keywords:
Activated carbon
Kinetics
Water adsorption
LDF model
Air flow
Relative humidity

Abstract

The performance of porous carbon materials as sorbents is often compromised by the presence of humidity. Studying the kinetics of water vapour adsorption on activated carbons will undeniably help to overcome this issue. This has been approached in this work by evaluating the influence of several operational factors on the dynamic adsorption of water vapour in these materials. Specifically, different carbon types, particle sizes, air flows and ambient conditions (temperature and relative humidity (RH)) were systematically investigated. The impact of each isolated parameter on both the maximum water uptake and the uptake rate was analyzed by fitting the experimental data to the Linear Driving Force (LDF) kinetic model. The results show that except for the particle size, the studied variables play a role in the water sorption kinetics, although to a different extent. It was also confirmed that the LDF model can adequately describe the kinetics of water vapour adsorption independently of the experimental conditions. Finally, the complete water vapour adsorption process can be described by this model, obtaining a different value of the kinetic constant for the sequential stages, involving different adsorption mechanisms.

1. Introduction

The study of water adsorption on activated carbons is very important since ambient humidity is present in most of the gas phase applications of these materials. Under real operating conditions, the water molecules from the surrounding atmosphere tend to infiltrate and occupy the adsorption sites reserved for other target molecules (e.g. organic vapours) or to influence the kinetics of the water vapour adsorption, thus compromising the performance of the carbon [1–4]. In this regard, while the mechanisms of water adsorption in carbon pores have been the subject of extensive research in the last years [5 and references therein], scarce works have been devoted to the study of the kinetics of adsorption [6–8].

*Corresponding author.
E-mail: leticia.fernandezvelasco@rma.ac.be

Thus, it has been established that water adsorption in nanoporous carbon materials is initialized by the interactions between the adsorbate and the surface groups attached at the edge of the graphene layers [9]. This is followed by additional adsorption on the initially adsorbed water molecules, which act as nucleation sites with the formation of 3D clusters [10]. As the relative pressure increases, these clusters grow and coalescence to fill the micropores [11]. The unique nature of this process would probably affect the kinetics of water vapour adsorption as well.

In this respect, most of the kinetic studies have been focused on the surface and textural properties of the carbon adsorbent [7–8, 12] and there is a general agreement that the rates of adsorption and desorption vary with the loading [5]. However, the effect of the operating conditions on the water sorption kinetics has not been properly addressed yet. In order to fill this gap, the carbon type and

other properties such as the air flow, particle size, temperature and relative humidity (RH), which may influence the dynamic adsorption of water, were investigated in this work. The contribution of each variable was isolated and the experimental results were correlated using the Linear Driving Force model (LDF).

2. Experimental

Two different commercial activated carbons, CGranular and R1 Extra (both Cabot Norit) were used in this study. They were selected based on their different textural and physico-chemical properties (Table 1). In order to evaluate the impact of the particle size on the water adsorption kinetics, two different particles sizes of CGranular were employed: 1–2 mm (sample CG1) and 0.5–0.8 mm (CG2).

The materials were characterized by means of nitrogen adsorption at -196 °C using an Autosorb-1 sorption device (Quantachrome Instruments). The isotherms were used to calculate textural parameters such as the BET specific surface area (S_{BET}), the micropore volume (by applying the Dubinin-Radushkevich equation), the total pore volume and the pore size distribution (slit-QSDFT kernel). Before each sorption measurement the activated carbons were outgassed at 120 °C for 24 h under vacuum. Water sorption isotherms at 20 °C were measured in a gravimetric water sorption analyzer (Aquadyne DVS, Quantachrome Instruments). The first part of the water adsorption isotherm was used to calculate the surface oxygen content by applying the equation described in [13]. A Quanta 400 (FEI Company) Scanning Electron Microscope (SEM) was used to visualize the morphology of the samples.

Contrary to organic vapour adsorption, there is no adsorption front in the case of water vapour adsorption [14–15]. This means that the breakthrough is immediate and therefore, the process needs to be followed gravimetrically. The humidified air passed through the activated carbon filter, which retained an amount of water that was translated into a gain in weight until saturation (the weight of the filter became stable). Thus, the samples were weighed at regular intervals to obtain a curve for weight gain versus time until a constant weight (+/- 0.025 g) was measured. All the dynamic adsorption experiments were conducted with the same bed height (4 cm) and with a filter diameter of 4.3 cm. Besides the nature of the carbon and the particle size, the other studied variables included air flow (10, 20 and 40 L/min), relative humidity (35, 65 and 85%) and temperature (20 and 40 °C). The latter parameters were only evaluated with sample CG1. The water vapour adsorption experiments were conducted on two test rigs, one that permits the control of relative humidity (RH) and airflow (at a fixed temperature) and a second one that allows to work at different temperature, but under fixed conditions of RH and airflow. More details about the specific conditions employed for each variable will be given in the subsequent corresponding sections.

3. Results and Discussion

3.1. Characterization of the materials

The SEM images of both carbons are presented in Fig. 1, revealing their different morphology. This can be explained by the distinct precursor and activation procedure followed for their preparation: whereas CGranular is obtained from wood by chemical activation, rendering a carbon with low apparent density, R1 is synthesized by the physical activation of peat. This also leads to a different porous structure, as it is discussed next.

The textural parameters presented in Table 1 show that R1 and CGranular displayed similar BET specific surface areas and consequently, micropore volumes, although being slightly lower for the former. In spite of this, the carbons display a different micropore size distribution (Fig. 2). Specifically, the size of the micropores of R1 is narrower, with a higher volume of ultramicropores (d<0.7 nm), while the volume of wide micropores is larger for CGranular. Furthermore, there is a marked

Table 1
Characteristics of the commercial activated carbons used in this study

Sample	Precursor	Shape	Particle size (mm)	S_{BET} (m^2/g)	$V_{micropores}$ (cm^3/g)	V_{total} (cm^3/g)	[O] (%)
CG1	Wood-based	Granular	1-2	1427	0.51	1.13	18.9
CG2		Granular	0.5-0.8	1409	0.46	1.13	18.9
R1	Peat-based	Extruded	0.5-5 length 0.8 diameter	1358	0.47	0.64	13.0

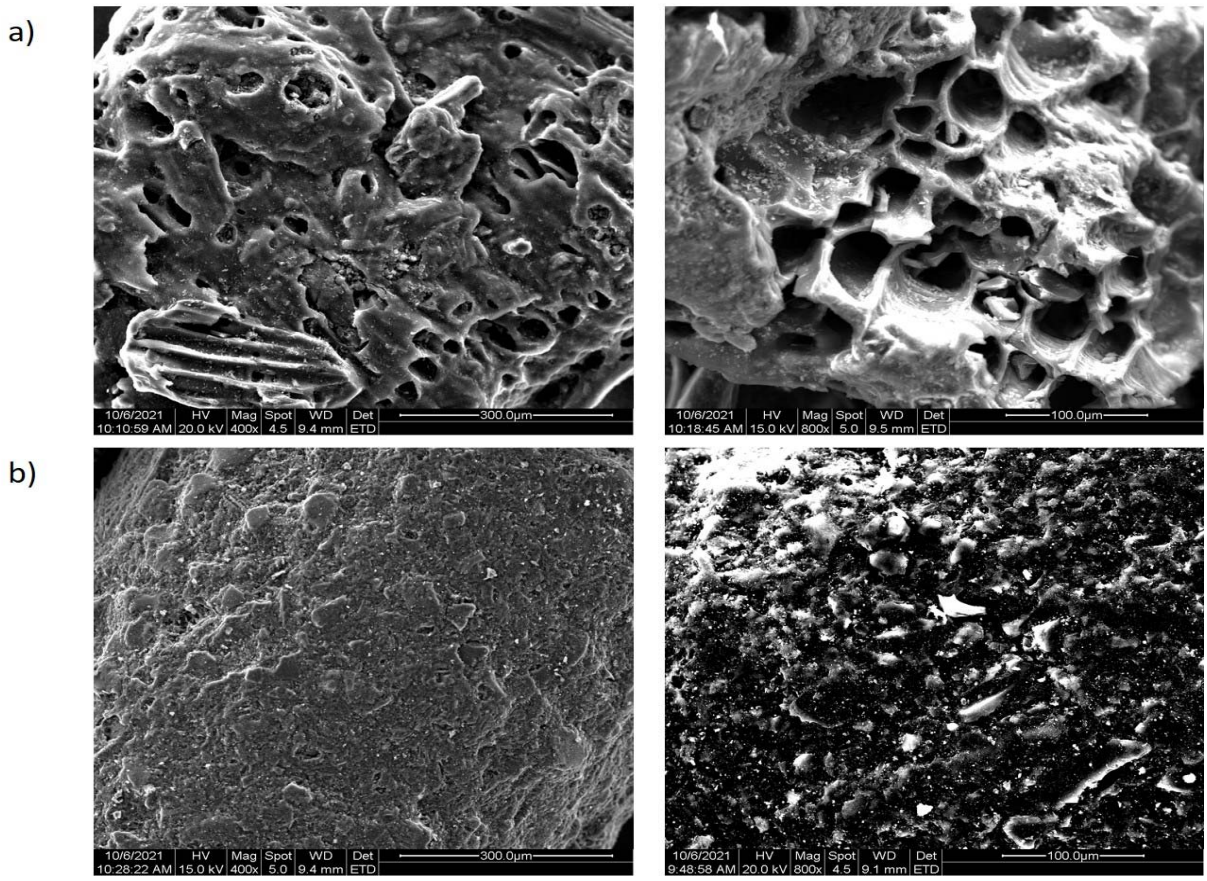

Fig. 1. SEM images of a) CGranular and b) R1 at two different magnifications (400 and 800x).

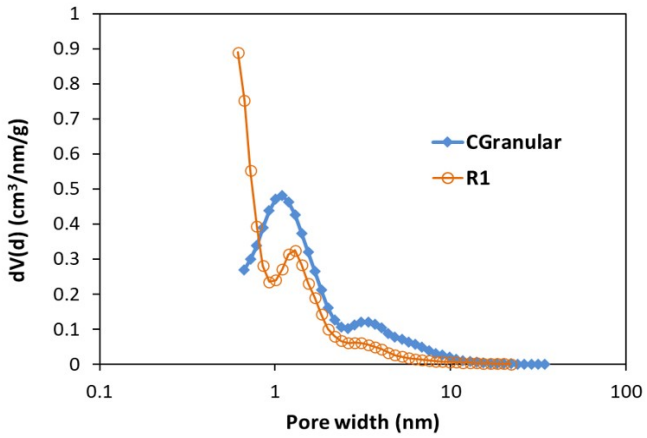

Fig. 2. Pore size distributions of carbons R1 and CGranular.

difference in the total pore volume, this indicating that while R1 is essentially a microporous carbon, CGranular has an important contribution of mesopores to the porous structure. This is also reflected in the pore size distributions of both carbons (Fig. 2). On the other hand, their differences in surface chemistry are highlighted by the higher surface oxygen content of CGranular, which was chemically activated. More precisely, the surface of CGranular is rich in carboxylic groups, as studied in a previous work by infrared and thermogravimetric techniques [16]. Sample R1 displays a similar thermogravimetric profile, but with a considerably lower mass loss. It is also important to note that the properties of CGranular were mostly preserved regardless of the particle size (CG1 and CG2).

The water vapour sorption isotherms of the activated carbons are plotted in Fig. 3. Both materials exhibit quite different adsorption profiles, it being linked with their particular textural and surface properties. The first region of the isotherm is dominated by the specific interactions between water and the surface oxygen functionalities. Thus, the slope of the curve is herein steeper for CGranular, with higher surface oxygen content. At higher relative humidities (RH), where water-water interactions prevail, there is a sharp raise of the curve, associated with the filling of the microporous system. The onset of the upswing is related to both the pore size and the surface chemistry of the material [5], being favored for more hydrophilic ones [17]. This is followed by the filling of the narrow mesopores at high relative humidities. In this last region, the curve is practically flat for R1 while it is still steep for CGranular due to its micro-mesoporous structure, reaching a much higher final water uptake.

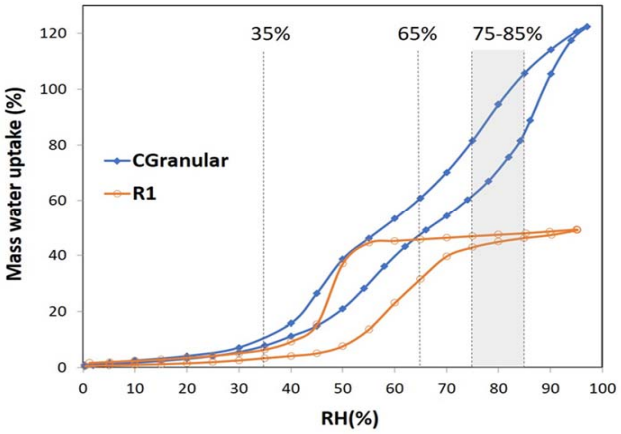

Fig. 3. Water vapour sorption isotherms at 20 °C of R1 and CGranular carbons. Vertical dotted lines indicate the relative humidities chosen for the kinetic study.

3.2. Kinetics of water adsorption

Among the various kinetic models for water adsorption described in the literature [5, 8], the Linear Driving Force model was applied for the correlation of the experimental results:

$$\frac{\Delta W(t)}{\Delta W\,max} = 1 - e^{-at}$$

where ΔW(t) is the mass gained as a function of time (g_{H2O}/g_{carbon}), ΔW_{max} is the mass gained at the saturation point (g_{H2O}/g_{carbon}) and a is the kinetic constant (min^{-1}).

This simple and versatile model is widely used to describe the adsorption kinetics of supercritical gases (such as nitrogen, oxygen, and argon) but it has also demonstrated its validity for water vapour on certain heterogeneous adsorbents such as activated carbons [6, 18–19].

In the next subsections, the influence of a range of factors on the water adsorption kinetics will be presented and discussed.

3.2.1. Carbon type

The first element to be evaluated was the carbon type. For this purpose, the tests were performed with samples R1 and CG1, with similar particle size. The rest of the parameters were fixed as follows: 20 L/min of air flow, 25 °C and 65% RH.

The obtained results are shown in Fig. 4a and Table 2. Therein, it is observed that carbon CG1 leads to a higher and faster adsorption of water vapour than R1. The first remark is in line with the water sorption isotherms (Fig. 3) and it is due to the more hydrophilic character and a more developed porous structure of CG1. Faster kinetics are illustrated by a steeper slope of the curve and the rapid reach of a plateau. On the contrary, the gain in weight for the R1 sample is steadier. In fact, the calculated kinetic constant is 3 times higher for CG1 (0.0067 vs 0.0215 min^{-1}). This behavior can be principally ascribed to the different textural properties of both carbons, and particularly to the more microporous nature of R1 and the abundance of narrow micropores. In this regard, it has been reported that the presence of pores of smaller size can retard the rate of diffusion and lead to much longer equilibration times [12, 20]. Moreover, the surface groups present on the surface of CG1 can enhance the rate of adsorption by providing nucleation sites for water clustering.

Finally, the goodness of fit of the LDF model to the experimental data seems to be acceptable, although some slight deviations are observed at the very first stages of the process, where equilibrium was not yet reached, and once the filter is saturated [21]. It is worth to note that the divergences are higher for the R1 carbon. This may be due to its more microporous nature, leading to longer equilibration times.

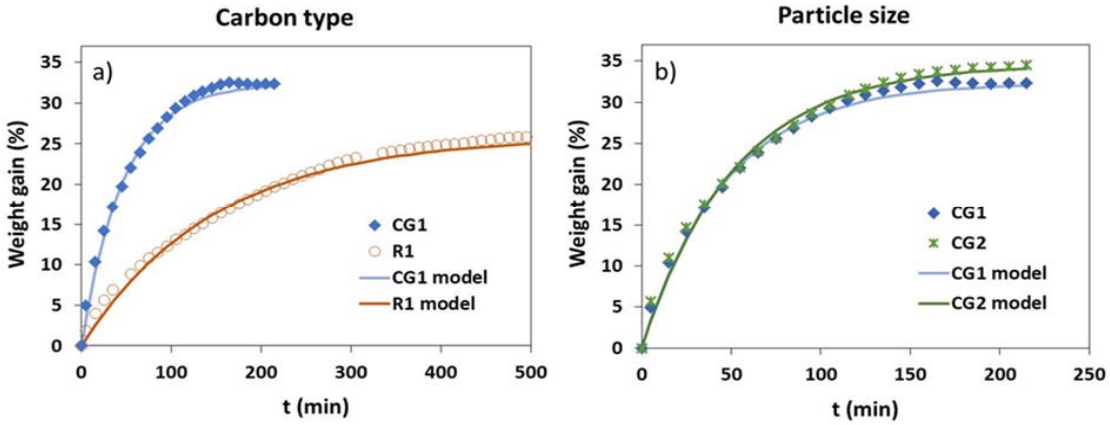

Fig. 4. Kinetics of water vapour adsorption as a function of a) carbon type and b) particle size.

Table 2
Kinetic parameters and goodness of fit obtained by applying the LDF model when studying the influence of the carbon type and the particle size

Sample	Kinetic parameters		
	a (min^{-1})	Maximum uptake (% weight)	R^2
CG1	0.0215	32.4	0.998
CG2	0.0195	34.6	0.997
R1	0.0067	25.9	0.997

Altogether, it is clear that the nature of the carbon plays a fundamental role on the adsorption kinetics of water adsorption.

3.2.2. Particle size

Then, CGranular carbon with different particle size (CG1 and CG2) was used to isolate the effect of this variable under the same operational circumstances indicated in 3.2.1.

The results gathered in Fig. 4b and Table 2 are very similar in both cases. Still, there is a slightly higher water uptake for the material of smaller grain diameter, which, on the contrary, exhibits a sensibly slower adsorption rate. This could a priori indicate that the particle size favours the total adsorption capacity while hardly hampering the adsorption kinetics. However, based on the characterization of the two carbons (Table 1), one would expect the opposite trend: a somewhat reduced capacity for CG2, showing less volume of micropores with the same surface oxygen content. Thus, bearing in mind the low degree of deviation and the plausible contribution of the experimental error, the influence of the particle size (if any) on the water sorption kinetics seems not to be significant.

3.2.3. Air flow

From this point in the study, the carbon type was fixed to CG1. Three different air flows were evaluated. 10, 20 and 40 L/min at 20 °C and 65% RH. The results are recorded in Fig. 5 and Table 3.

First, a direct relation between the air flow and the adsorption rate is noticed. This can be explained by an increased pressure through the filter when raising the air flow, thus contributing to increase the concentration gradient and therefore, the mass transfer within the pores. Also, a higher linear velocity through the filter will enhance the interparticle diffusion. Consequently, the sorption kinetics will be accelerated. Nonetheless the impact of this

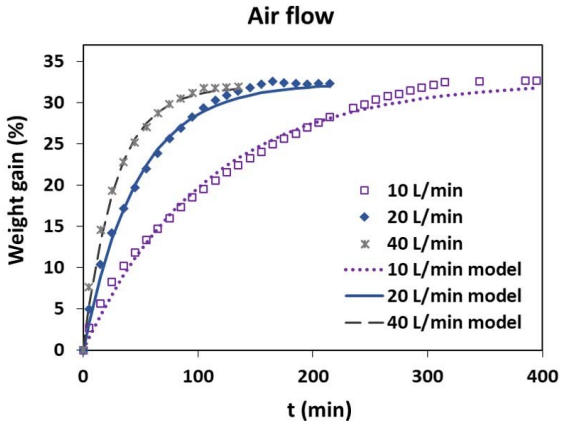

Fig. 5. Kinetics of water vapour adsorption on CG1 as a function of the air flow.

Table 3
Kinetic parameters and goodness of fit obtained by applying the LDF model when studying the effect of the air flow

Sample	Air flow (L/min)	Kinetic parameters		
		a (min^{-1})	Max. uptake (% weight)	R^2
CG1	10	0.0093	32.7	0.995
	20	0.0215	32.4	0.998
	40	0.0360	31.9	0.997

variable on the kinetics is gradually reduced as the air flow is increased. In this manner, the increase in the kinetic constant is higher from 10 to 20 L/min (2.3 times) than from 20 to 40 L/min (1.7 times), as it can be clearly seen in the graph. A second interesting observation is that the total capacity of the carbon towards water keeps constant (32%) regardless of the air flow used.

Finally, the fitting of the LDF model is once again satisfactory, and even more accurate when the air flow is increased. This trend indicates again that the equilibration time has an influence on the accuracy of the model.

Summarizing, it can be concluded that the air flow has an important effect on the water adsorption rate but not on the total capacity.

3.2.4. Relative humidity

Next, the experiments were performed at three different relative humidities: 35, 65 and 85% with an air flow of 20 L/min and at 20 °C. These RH values were not randomly chosen but based on the existence of three differentiate regions in the water sorption isotherms (Fig. 3), accounting for different adsorption phenomena as previously explained.

Logically, the maximum water uptake of the carbon (Table 4 and Fig. 6a) becomes higher with increasing the relative humidity used. Regarding the kinetics, the rate of adsorption at 35% RH is much higher than at 65 and 85%, obtaining much closer values for these latter two, where the filling of the micropores and narrow mesopores takes place. Besides the fact that a higher quantity of water vapour will require a longer time to be adsorbed in the carbon, the different mechanisms involved in the water sorption process also play a role in the kinetics. At low relative pressures (35%) the adsorption rate is fast because the water molecules are still building up around the surface oxygen functional groups [5]. However, as the water sorption process proceeds, the filling of the pores starts to take place. In this regard, it is assumed that the slowest step in water adsorption is related to the formation of water molecular assemblies [8, 19, 22]. Thus, the kinetic rates at 65 and 85% will be both mainly determined by the pore filling and consequently be slower. The slightly lower value at 85% is due to the filling of a somewhat higher fraction of the pore network of the activated carbon.

The theoretical model overlaps the experimental data successfully for the three RHs tested, thus meaning that even if the adsorption mechanism at each RH is different, they all obey the LFD equation. It is worth of note that the goodness of fit close to saturation is directly related to the value of the kinetic constant.

3.2.5. Temperature

Finally, the influence of the temperature was assessed. In this case, the experiments were realized at 20 and 40 °C, 75% RH and 40 L/min of air flow and the data are compiled in Table 4 and Fig. 6b.

As expected, the total water uptake decreases while raising the temperature. This is due to the exothermic character of the adsorption process and to the hindering of the formation of water clusters by significant thermal fluctuations at higher temperatures [5]. Contrarily, the kinetic constant increases with the temperature. In this case, this is linked with an increased diffusivity. The Knudsen diffusivity can be disregarded in the actual experimental conditions due to the high air flow used. However, the inter- and intra- particle diffusion coefficients will directly increase with the temperature and therefore, boost the velocity of the process [18, 23].

The experimental data follow a linear driving force mass-transfer rate law for most of the

Table 4
Kinetic parameters and goodness of fit obtained by adjusting the experimental data with the LDF model when varying the relative humidity or the temperature

Sample	RH (%)	Kinetic parameters			T (°C)	Kinetic parameters		
		a (min^{-1})	Max. uptake (% weight)	R^2		a (min^{-1})	Max. uptake (% weight)	R^2
CG1	35	0.0750	6.0	0.987	20	0.027	31.9	0.992
	65	0.0215	32.3	0.997	40	0.032	23.9	0.996
	85	0.0195	52.7	0.998				

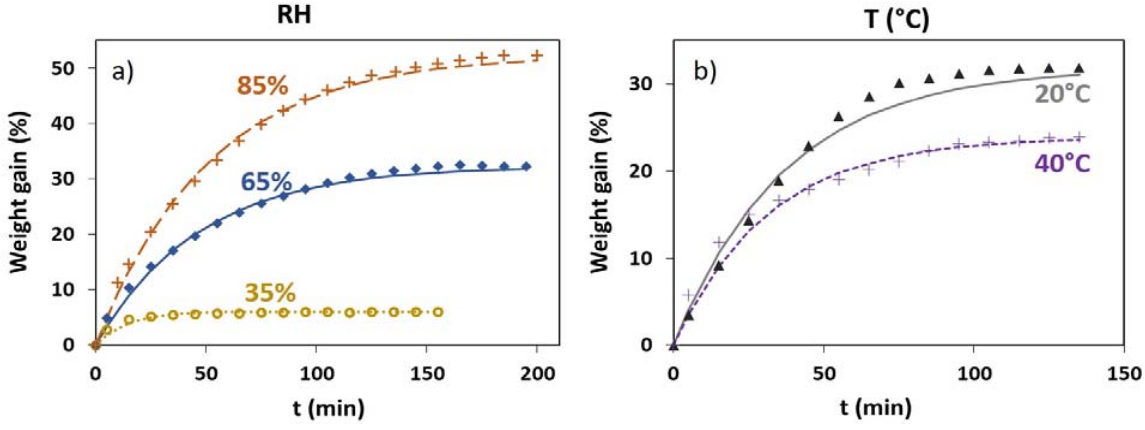

Fig. 6. Kinetics of water vapour adsorption on CG1 as a function of a) RH and b) T.

adsorption process. However, and interestingly, the theoretical curves obtained by the LFD model underestimate the experimental data at different stages of the adsorption process depending on the temperature: close to saturation for 20 °C and initially for 40 °C.

4. Conclusions

A better understanding of the water adsorption kinetics in activated carbons is fundamental in order to enhance the performance of these materials in a wide range of applications. In this work, several experimental parameters were modified in order to study their impact on the water sorption kinetics. Among them, the ones having the highest effect were the carbon textural and surface properties and the environmental parameters (temperature and relative humidity). The air flow has an important influence on the adsorption rate but not on the maximum water uptake. On the contrary, the particle size does not seem to have a relevant effect.

It was also confirmed that the Linear Driving Force model can adequately describe the kinetics of water vapour adsorption independently of the experimental conditions. Moreover, the three steps of water vapour adsorption, involving different mechanisms, may be described by this model using a different kinetic constant for each mechanism.

5. Acknowledgements

The authors wish to thank Cabot Norit who kindly provided them with the activated carbon samples. We are grateful to Laurent Evrard and Prof. Rabet (MECA department, RMA) for the SEM images.

References

[1]. A. Toth, K. Laszlo, Water adsorption by carbons. Hydrophobicity and hydrophilicity, Novel carbon adsorbents, Editor J.M.D. Tascon, Elsevier, Oxford, UK, 2012, p. 147. DOI: 10.1016/B978-0-08-097744-7.00005-3

[2]. F. Cosnier, A. Celzard, G. Furdin, D. Bégin, J.F. Marêché, *Adsorpt. Sci. Technol.* 24 (2006) 215–228. DOI: 10.1260/026361706778812871

[3]. P. Lodewyckx, E.F. Vansant, *Am. Ind. Hyg. Assoc. J.* 60 (1999) 612–617. DOI: 10.1080/00028899908984480

[4]. P. Lodewyckx, L.F. Velasco, Y. Boutillara, *Eurasian Chem.-Technol. J.* 21 (2019) 193–201. DOI: 10.18321/ectj860

[5]. L. Liu, S.J. Tan, T. Horikawa, D.D. Do, D. Nicholson, J. Liu, *Adv. Colloid Interfac. Sci.* 250 (2017) 64–78. DOI: 10.1016/j.cis.2017.10.002

[6]. N.J. Foley, K.M. Thomas, P.L. Forshaw, D. Stanton, P.R. Norman, *Langmuir* 13 (1997) 2083–2089. DOI: 10.1021/la960339s

[7]. A.J. Fletcher, Y. Uygur, K.M. Thomas, *J. Phys. Chem. C* 111 (2007) 8349–8359. DOI: 10.1021/jp070815v

[8]. H. Ito, T. Iiyama, S. Ozeki, S, *J. Phys. Chem. C* 119 (2015) 4118–4125. DOI: 10.1021/jp5118085

[9]. M.M. Dubinin, V.V. Serpinsky, *Carbon* 5 (1981) 402–403. DOI: 10.1016/0008-6223(81)90066-X

[10]. E.A. Muller, L.F. Rull, L.F. Vega, K.E. Gubbins, *J. Phys. Chem.* 100 (1996) 1189–1196. DOI: 10.1021/jp952233w

[11]. D.D. Do, H.D. Do, *Carbon* 38 (2000) 767–773. DOI: 10.1016/S0008-6223(99)00159-1

[12]. P. Lodewyckx, *Carbon* 48 (2010) 2549–2553. DOI: 10.1016/j.carbon.2010.03.032

[13]. P. Lodewyckx, E. Raymundo-Pinero, M. Vaclavikova, I. Berezovska, M. Thommes, F. Béguin, G. Dobos, *Carbon* 60 (2013) 556–558. DOI: 10.1016/j.carbon.2013.04.006

[14]. L. Richelet, Mesure de la cinétique de l'adsorption de la vapeur d'eau par les filtres de masques anti-gaz, Master Thesis for the degree of Master of Science in Engineering, Royal Military Academy, Belgium (2018).

[15]. P. Lodewyckx, S. Blacher, A. Léonard, *Adsorption* 12 (2006) 19–26. DOI: 10.1007/s10450-006-0135-2

[16]. L.F. Velasco, A. Devos, P. Lodewyckx, *Carbon* 152 (2019) 409–415. DOI: 10.1016/j.carbon.2019.06.054

[17]. S.S. Barton, J.E. Koresh, *J. Chem. Soc. Faraday Trans.* 79 (1983) 1147–1155. DOI: 10.1039/F19837901147

[18]. L. Jia, X. Yao, J. Ma, C. Long, *Micropor. Mesop. Mat.* 241 (2017) 178–184. DOI: 10.1016/j.micromeso.2016.12.028

[19]. A.W. Harding, N.J. Foley, P.R. Norman, D.C. Francis, K.M. Thomas, *Langmuir* 14 (1998) 3858–3864. DOI: 10.1021/la971317o

[20]. S. Diallo, *Phys. Rev. E* 92 (2015) 012312. DOI: 10.1103/PhysRevE.92.012312

[21]. M.J. Rupa, A. Pal, S. Mitra, B.B. Saha, *Chem. Eng. J.* 420 (2021) 129785. DOI: 10.1016/j.cej.2021.129785

[22]. L.F. Velasco, K.H. Kim, Y.-S. Lee, P. Lodewyckx, *Front. Chem.* 8 (2021) 593756. DOI: 10.3389/fchem.2020.593756

[23]. D.D. Duong, Adsorption analysis: equilibria and kinetics, Imperial College Press, Queensland, 1998.